Chem. Chem. Technol., 2023,
Vol. 17, No. 4, pp. 857–869

Chemical Technology

PREPARATION AND CHARACTERIZATION OF RED MUD-BASED GEOPOLYMER COMPOSITED WITH RICE HUSK ASH FOR THE ADSORPTION OF BROMOCRESOL GREEN IN AQUEOUS SOLUTION

***Khoa Dang Nguyen*[1, ✉], *Anh Thi Hoang Tran* [1], *Noor Haida Mohd Kaus*[2]**

https://doi.org/10.23939/chcht17.04.857

Abstract. Geopolymer-based industrial waste as red mud (RM) was successfully obtained in the presence of different loadings of rice husk ash (RHA). During the preparation, the added amounts of RHA in the geopolymer composition were varied from 10 to 50 % when the mass ratio of binder solution (Na_2SiO_3) and activated alkali-metal solution (NaOH 7 M) were 2.5 and the curing condition was fixed at 333 K within 24 h. For characterization, the surface morphology was evaluated by scanning electron microscope (SEM) equipped with the energy-dispersive X-ray, which detected the distribution of elements before and after the geopolymerization. To indicate the formation of geopolymer, Fourier–transform infrared spectroscopy (FT-IR) was used. The effect of the loading amounts of RHA on the Brunauer–Emmett Teller (BET) surface area value and Barrett–Joyner–Halenda (BJH) pore size of the obtained geopolymers were determined using a nitrogen gas adsorption instrument. In the bromocresol-green (BG) adsorption performed at pH 2, the higher addition of RHA in the geopolymer composition enhanced the adsorption capacities within 180 minutes. In addition, the adsorption behavior of the mixed geopolymer to BG fits well the Langmuir model, indicating that the adsorption occurs on the homogeneous monolayer surface of geopolymer. From this study, the RHA could be a natural potential filler to improve the BG-uptake of RM-based geopolymer in wastewater treatment.

Keywords: dye adsorption, geopolymer, bromocresol green, red mud, rice husk ash.

[1] Faculty of Environment, School of Technology, Van Lang University, Ho Chi Minh City, 70000, Vietnam
[2] School of Chemical Sciences, Universiti Sains Malaysia, Penang, 11800, Malaysia
✉ *khoa.nd@vlu.edu.vn*

1. Introduction

Textile production is one of the most polluting industries. Production processing generates a lot of pollutants such as wastewater, waste heat, solid waste, and exhaust gas from dryers, as well as gas emissions from boiler plants in which wastewater is an important problem facing the textile sector.[1] Depending on different factors such as the type of production processing and the used dyes, the parameters of the obtained wastewater are varied in terms of quantity and quality.[2] According to the document of Vietnam Textile Industry, it might consume approximately 200 to 1,000 kg chemicals and auxiliaries to produce one ton of product. In the case of dyes, this amount for one ton product is from 20 to 80 kg. However, the use efficiency is 70-80 %, which means that the remaining 20-30 % is about to be discharged into the environment.[3] According to the Ellen Macarthur Foundation, each year the textile industry consumes about 93 billion cubic meters of water.[4] In recent years, the contribution of the textile and dyeing industry to economic development has been significant and undeniable. Nevertheless, most of the factories of textile dyeing enterprises do not have wastewater treatment systems and tend to discharge directly into outside receivers. This type of wastewater has alkalinity, high color, and contains many chemicals that are toxic to aquatic species.[5,6] Therefore, the dye-contained wastewater must be strictly treated before being discharged into the environment. It has been known that various methods can be applied for dye elimination in aqueous solutions. Conventional physical dye removal methods include ion exchange, coagulation or flocculation, and filtration techniques such as nano/ ultra-filtration and reverse osmosis.[7] However, adsorption might have more potential due to its simplicity and high efficiency using low-cost materials.[8] In this study, we would like to propose a regenerated adsorbent called geopolymer.[9]

The definition of geopolymer proposed by Davidovits in the 1970s was an inorganic aluminosilicate polymer synthesized by the reaction of an aluminosilicate compound and an alkaline solution at high concentration.[10] Aluminosilicate binders or inorganic polymeric compounds resulted from a polycondensation reaction where a three-dimensional tecto-aluminosilicate matrix was obtained.[11] Silicate is regarded as a silicon-oxo-aluminate unit, the network of which consists of SiO_4 and AlO_4 tetrahedra linked by sharing all oxygen atoms through covalent bonds. The presence of cations such as Na^+ or K^+ maintains the balance of the remaining anions of the four-coordinated Si^{4+} and Al^{3+} ions.[12] It has been reported that the concentration of the alkali-metal solution used in the geopolymerization can vary depending on specific purposes. However, most studies propose that the alkali concentration might be high (5-15M) [13] to involve the geopolymerization,[14] in which geopolymer activated with NaOH solution was able to be improved in terms of compressive strength relative to KOH solution at the same concentration.[15] In addition, due to hydration and shrinkage, the strength is able to be decreased after curing at temperatures above 353 K owing to the disruption in the geopolymer structure.[16] The geopolymer process was most efficient at temperatures between 333-353 K [17] and the mass ratio of Na_2SiO_3/NaOH was about 2.5. [18] The increment in alkali-activated solution and the addition of binder as sodium silicate (Na_2SiO_3) can enhance the properties of the prepared geopolymer in terms of mechanical strength.[10,19]

Various synthesis methods were used to react an aluminosilicate precursor with activated chemicals to proceed with the geopolymerization.[20] The initial material having aluminosilicate contents could be natural mineral compounds or industrial waste, such as red mud (RM). The alkaline condition was commonly selected since it was well-suitable for RM due to its highly pristine alkalinity. The chemical compositions of RM differed depending on typical processes including Al_2O_3, Fe_2O_3, and SiO_2 in various percentages.[21] However, the low content of SiO_2 in RM limited the preparation of RM-based geopolymer. Normally, RM has been known as a supporting material in the geopolymerzation process. However, the aim of this study is to increase the geopolymerization from RM and improve the dye-adsorption performance of RM-based geopolymer. Hence, another natural additive, rice husk ash (RHA), was used as an alternative. RHA filler was derived from rice husks after being burnt in the open air outside the rice mill. It was usually an agricultural waste or an environmental problem.[22] The main chemical component of RHA is an amorphous silica oxide which was not only used as a silica supplement but also increases the removal efficiency.[23]

The aim of this research was to prepare the RM-based geopolymer at different loading amounts of RHA in the presence of an activated binder and highly concentrated alkali solutions. The concentration of the NaOH aqueous solution was fixed at 7 M due to the pristine alkalinity characteristic of red mud. The ratio between the alkali solution and the binder was used as 2.5. After the geopolymerization, the resulting samples were evaluated for their morphologies and element distribution using SEM-EDS, the surface area using BET surface areas, and Zeta-potential to estimate the surface-charge for the simulating adsorption of bromocresol green (BG) in aqueous solutions (Fig. 1).

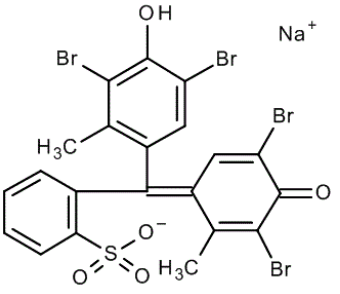

Fig. 1. The chemical structure of bromocresol green

2. Experimental

2.1. Materials

Red mud (RM) used in this study was locally collected from Lam Dong Provine, Vietnam while rice husk ash (RHA) was obtained from Long An Province, Vietnam. Other chemicals such as sodium hydroxide (NaOH, 99 %) and sodium silicate (Na_2SiO_3, SiO_2: 28.5 % and Na_2O: 8.5 %) and bromocresol green (BG) were purchased from Merck, Germany. All chemicals used in the preparation of geopolymer, and adsorption test were of analytical grade.

The RM (Fig. 2a) and the RHA (Fig. 2b) were ground and sieved through a 245-μm sieve, followed by washing in water and drying at 378 K in 24 h. The main components of RM and RHA were determined using an X-ray fluorescence (XRF) instrument (ZSX Primus II; Rigaku Corp., Japan) as presented in Table 1.

a) b)

Fig. 2. Appearance of RM a) and RHA b)

Table 1. The main chemical components (%) of RM and RHA

Samples	The main components (%)				
	SiO_2	Al_2O_3	Fe_2O_3	CaO	TiO_2
RM	0.74	37.8	44.2	0.24	8.14
RHA	87.2	0.32	0.24	1.79	-

Table 2. The mixture proportions of initial materials, BET surface area, BJH pore volume and size of the obtained geopolymers

Sample	Proportion (g per 100 g)				Si content (%)	Surface area (m^2/g)	BJH pore volume (cm^3/g)	BJH pore size (nm)
	RM	RHA	Na_2SiO_3	NaOH 7 M				
RM	-	-	-	-	0.27	25.6	0.04	6.3
10 %	46.0	5.1	35	14	7.20	26.5	0.05	6.8
30 %	35.7	15.3	35	14	9.72	27.3	0.04	6.2
50 %	25.5	25.5	35	14	26.0	31.1	0.05	6.0
RHA	-	-	-	-	39.5	9.69	0.01	5.1

2.2. Methods

2.2.1. Preparation of the geopolymer composites

The pre-treated RM and RHA were mixed with the appropriate amount of 7M NaOH and Na_2SiO_3 aqueous solution. Here, the mass ratio between Na_2SiO_3/NaOH was kept at 2.5. [10] The loading of RHA in the geopolymer composition was varied at 10 %, 30 %, and 50 % (Table 2). The paste was mixed for 10 minutes at room temperature before being poured into a cubic-plastic container ($50 \times 50 \times 50$ mm^3) and dried at 333 K. After 24 hours, the geopolymers were obtained. Before measurements, all samples were ground and sieved through a 245-µm sieve followed by washing in the excess amount of deionized water until pH reached a neutral value. The geopolymers were labeled according to the weight percentage of the added amounts of RHA. For example, the geopolymer prepared with 90 % RM and 10 % RHA was 10 %. The appearance of the geopolymers prepared from RM and RHA is shown in Fig. 3.

2.2.2. Characterization of the geopolymer composites

The surface morphologies of the samples were observed using scanning electron microscopy (SEM) (JSM-IT300, JEOL, Japan) - Energy dispersive spectrometer (EDS) JSM-5300LV; JEOL Ltd., Japan). Fourier transform infrared spectroscopy (FT-IR) was performed using a JASCO FT-IR/4100 spectrometer by grinding the dried samples with potassium bromide (KBr). X-ray fluorescence (XRF) instrument (ZSX Primus II; Rigaku Corp., Japan) was used to determine the differences in elemental content after the geopolymerization process. The–Brunauer–Emmett Teller (BET) surface area and Barrett–Joyner–Halenda (BJH) pore size distribution of the obtained geopolymers were determined using a nitrogen gas adsorption instrument (TriStar II 3020; Micromeritics Instrument Corp., USA) at 77 K. To determine the surface-charged of the geopolymers at different pH solutions, Zeta potential was used by Zeta-potential analyzer (ELSE1NGK; Otsuka Electronics Co. Ltd., Japan).

2.2.3. The adsorption experiment of bromocresol green aqueous solution

The stock dye solutions of 1000 mg/L were prepared by dissolving BG in deionized water at pH 2.[24,25] The adsorbent mass of the prepared geopolymer was 0.10 g placed in 20 mL of BG solutions from 20 to 120 mg/L. The mixtures were stirred for 180 minutes at 200 rpm and 273 K. Afterwards, the sample was centrifuged at 3000 rpm for 10 min. The initial and residual concentrations were measured using a UV-Vis spectrophotometer (V-750, Jasco, Japan) at a wavelength of 423 nm for BG. The removal efficiency of the geopolymers was calculated using Eq. (1), and adsorption capacity at any time q_t (mg/g) and adsorption capacity at equilibrium q_e (mg/g) were determined using Eq. (2).

The removal percentage (H %) was:

$$H(\%) = \frac{C_0 - C_t}{C_0} \times 100 \quad (1)$$

where H was the removal capacity of the dyes adsorbed (%), C_o and C_t were the initial and the time concentration of dyes in the solution (mg/L), respectively.

The adsorption amount of BG at the current time (q_t, mg/g) and equilibrium adsorption capacity (q_e, mg/g) were calculated according to the following equations:

$$q_{t,e} \frac{\left(C_0 - C_{t,e}\right) \cdot V}{M} \quad (2)$$

where C_o and C_t (mg/L) are the concentrations of the solution at the initial time and time t (h), respectively; C_e (mg/L) is the equilibrium concentration of dye solution; V (L) is the volume of the contaminated solution and m (g) is the weight of the dried adsorbent.

3. Results and Discussion

3.1. Appearance of the Prepared RM and RHA-Based Geopolymer Composites

Fig. 3 represented images of the obtained geopolymer composites with varying amounts of RHA from 10 to 50 %. It was observed that the color of the obtained geopolymers changed as the amount of RHA increased, gradually shifting from dark orange for 10 % to light brown for 50 % of RHA. The geopolymers with 10 % and 30 % RHA displayed fractures on the surface due to the loss of water during the curing process. In the case of the 50 % of RHA in the geopolymer composition, the distribution of RHA powder was observed. As listed in Table 2, the Si content varied between the prepared geopolymers. The 10 % RHA sample contained 7.2 % Si, while the 50 % RHA geopolymer had a significantly higher Si content of around 26 %.

a) b) c)

Fig. 3. Images of the prepared geopolymer composites a) 10 %, b) 30 % and c) 50 %

3.2. Appearance of the prepared RM and RHA-based geopolymer composites

3.2.1. Morphological measurements and element distribution detection

The morphologies of the prepared geopolymer composite with different mixing amounts of initial materials as RM, RHA are shown in Fig. 4. At the magnification of 500× (Fig. 4a), the morphology of RM was observed in various shapes and sizes. Moreover, the impurity was observed on the surface of the RM particle at a magnification of 2000×. In Fig. 4e, the porous structure was obtained on the surface of RHA particles. For the RM-RHA based geopolymer, the surface of the prepared particles appeared more porous in the case of 10 % RHA-adding (Fig. 4b at 2000×). When the higher loading amount of RHA at 50 % was used in the geopolymer preparation, a large number of tiny particles were observed (Fig. 4d). This might be due to the fact that RHA powders were well-dispersed in the geopolymer structure. In order to confirm this observation, the element distributions of components are shown in Fig. 5 and the percentage in Table 3.

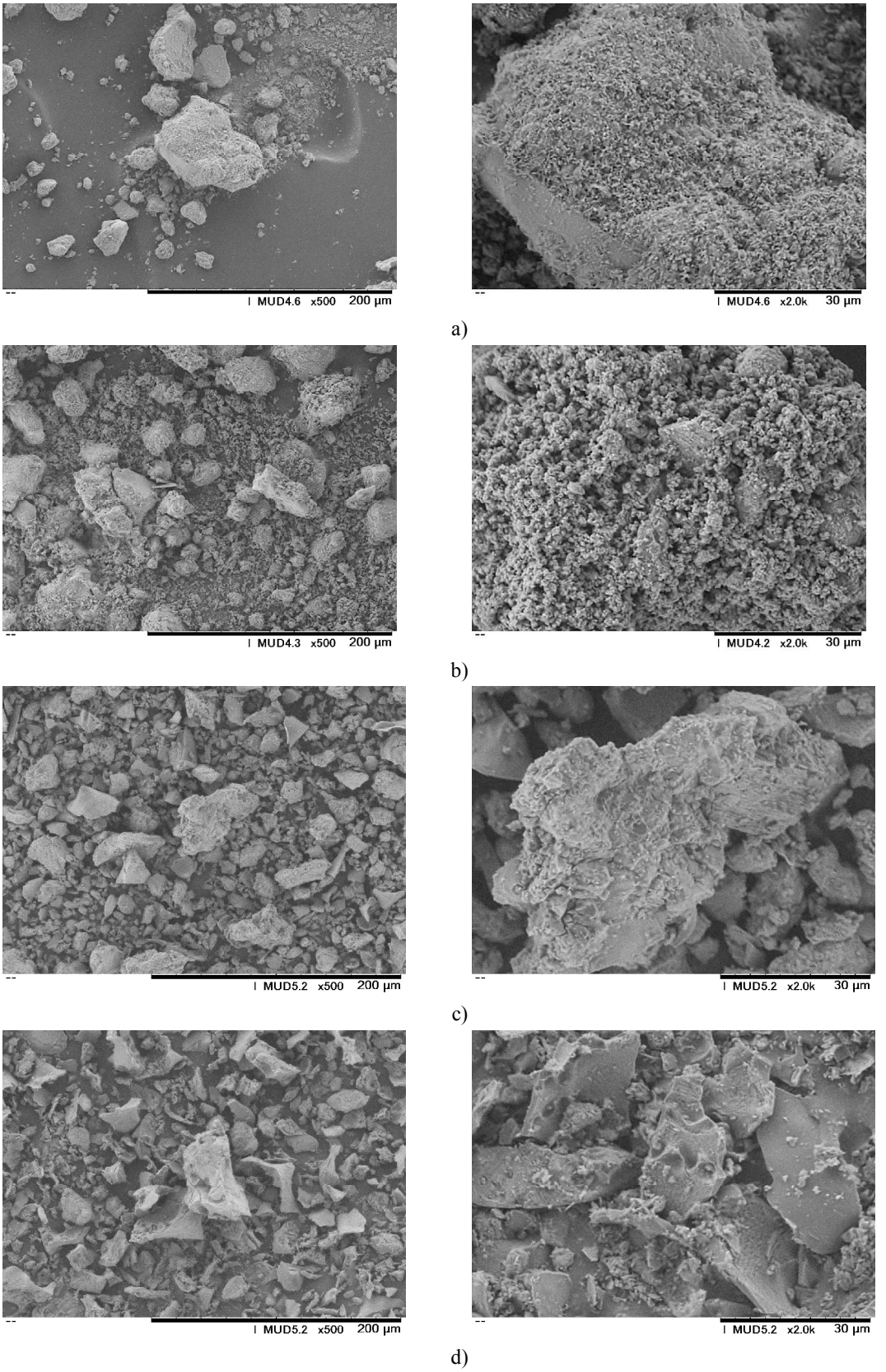

Fig. 4. SEM images of the initial materials RM: a), prepared geopolymer composites 10 % – b), 30 % – c), 50 % – d)

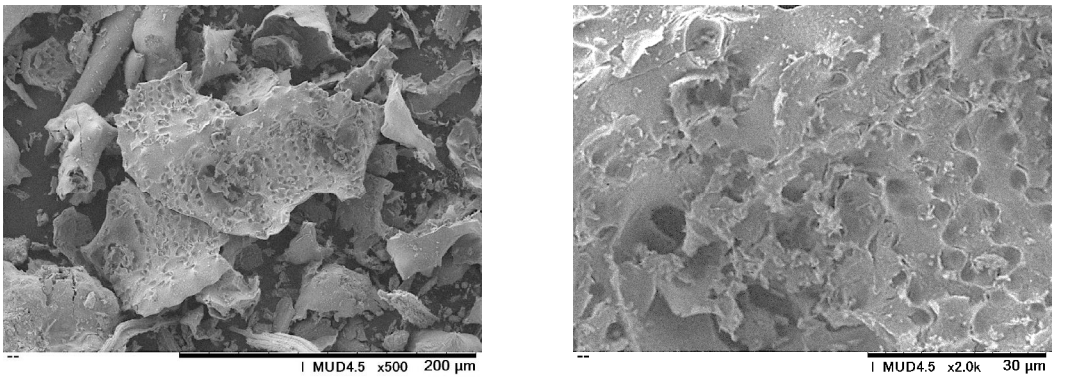

e)

Fig. 4. SEM images of the initial materials RM: and RHA – e) at magnification of 500× (left) and 2000× (right)

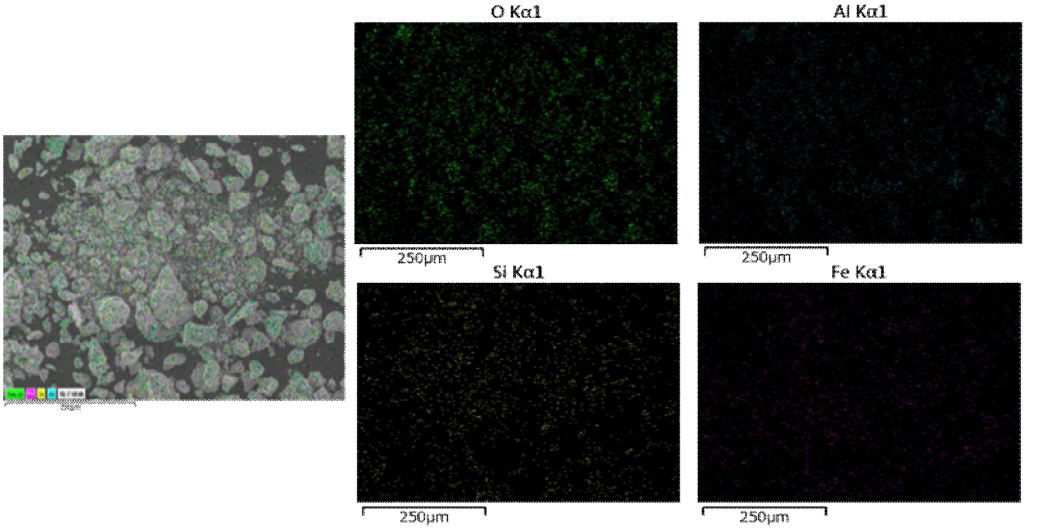

a)

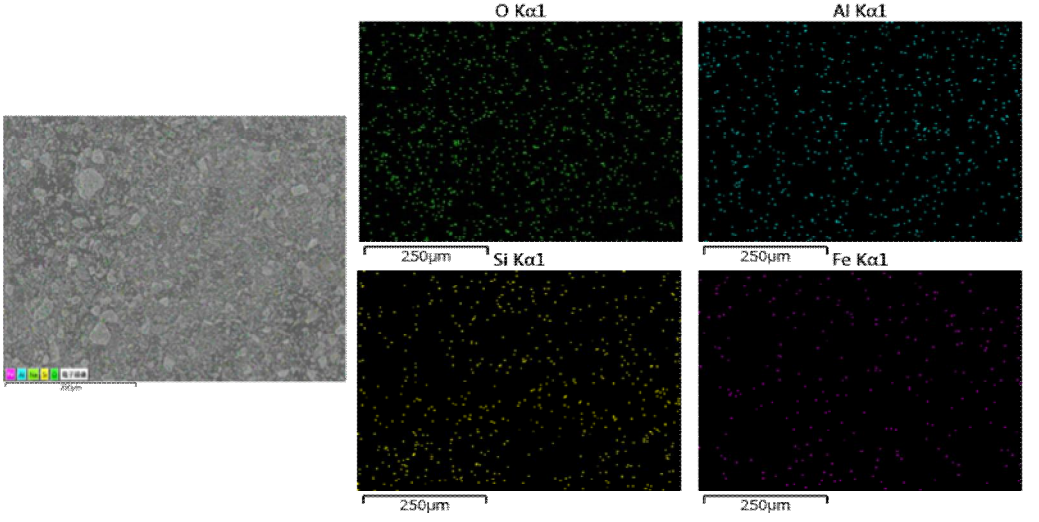

b)

Fig. 5. SEM-EDS mapping of geopolymer composites: a) 10 %; b) 30 %

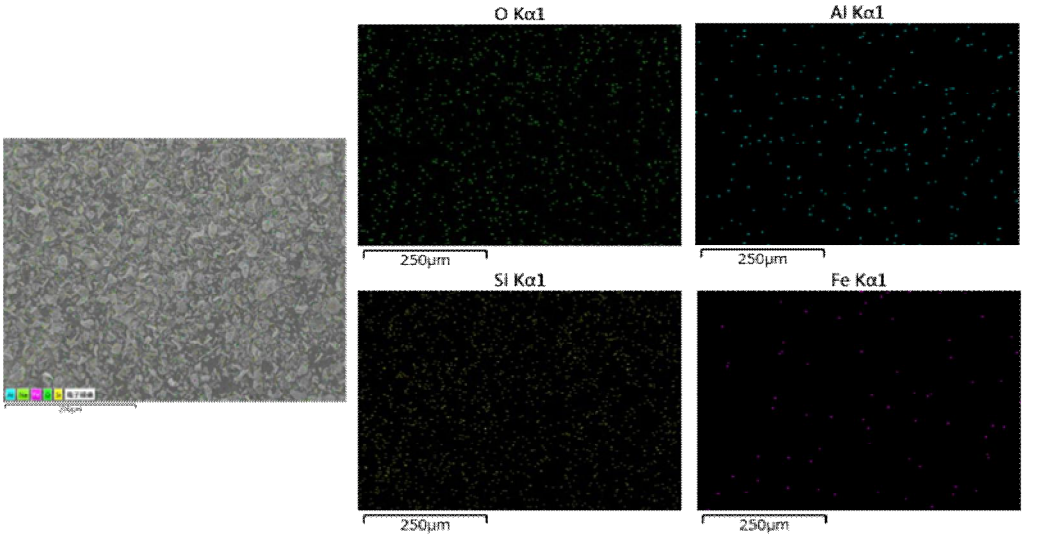

c)

Fig. 5. SEM-EDS mapping of geopolymer composites: c) 50 %

Table 3. Main element content (%) from EDS mapping

Sample	Main element content (%) from EDS mapping				
	Si	Al	Fe	O	Na
10 %	8.40	15.2	25.9	48.6	2.00
30 %	13.8	12.8	21.4	52.1	0.00
50 %	34.3	3.70	9.9	56.4	0.00

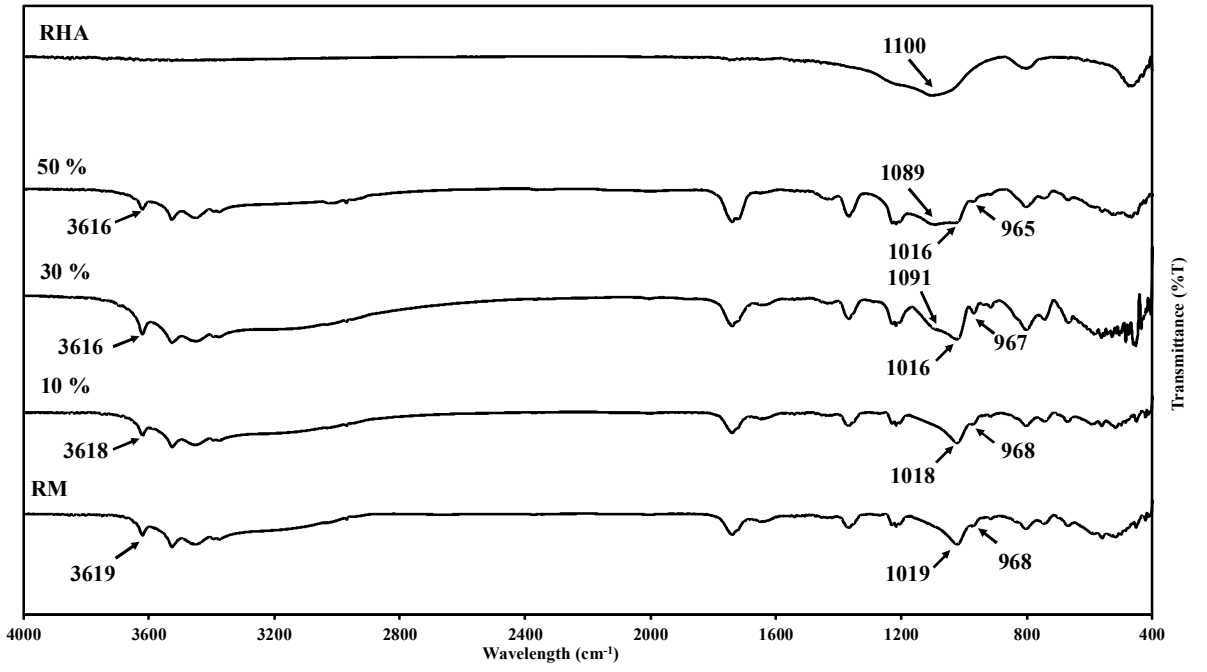

Fig. 6. FT-IR spectra of the initial materials and prepared geopolymer composites

3.2.3. FT-IR spectrum

As seen in Fig. 6, mostly in all the spectra of RM and the geopolymers, the hydroxyl-stretching band was presented in the region at 3450–3400 cm^{-1} wavelengths indicating the formation of hydrogen-bonded surface OH groups. The absorption peak near 3620 cm^{-1} was assigned to the inner-hydroxyl groups.[26] The band at the wavelength of 1736–1726 cm^{-1} represented the double bond of the C=O group, whereas the band detected at 1630 cm^{-1} was attributed to the bending vibration of H–O–H occluded inside the aluminosilicate structure.[27] The characteristic band of Si–O was also observed at 968 cm^{-1} in the case of RM. However, this wavelength was shifted to be lower at 967 and 965 cm^{-1} with the added RHA of 30 and 50 % during the geopolymerization. The position of the Si–O–T (T= Si or Al) asymmetric stretching band located at 1019 cm^{-1} was found to shift to the lower wavelength of 1018, 1016, and 1016 cm^{-1} when the RHA amount was added of 10, 30, and 50 % in the geopolymer content, respectively.[26] Moreover, the band of O–Si–O stretching at 1100 cm^{-1} in RHA was lightly shifted to 1089 and 1091 cm^{-1} in the case of 50 % and 30 % RHA, respectively.[28] In addition, these peaks in the geopolymer structure were broader than those of RHA. This evidence suggested that the initial materials were well-interacted with the additives, and the formation of geopolymers between RM and RHA was confirmed.

3.2.4. BET surface area and BJH determination

The nitrogen adsorption/desorption isotherm of samples was illustrated in Fig. 7. It could be observed that the initial RM and the geopolymer composite were composed of mesoporous structure followed as type IV at which pore width was greater than 4 nm.[29] Meanwhile, the RHA was strongly considered to be type V distinguished by its characteristic S-shaped isotherm.[30] However, all samples were subjected to mono and multiple adsorption with capillary condensation[31] after the geopolymerization, the surface area of the 10 % RHA-containing geopolymer was increased to 26.5 m^2/g, which was higher than those of RM (25.6 m^2/g) and RHA (9.69 m^2/g). The reason was that the activation by concentrated sodium hydroxide solution could strongly interfere with the surface of the geopolymer particles. In fact, higher RHA contents in the preparation of RM-based geopolymer increased the surface area of the resultant geopolymers. The surface area values of the geopolymer sample prepared at 50 % RHA were improved to 31.1 m^2/g. The BJH results showed that the pore volume remained unchanged at different RHA concentrations. Meanwhile, the BJH pore size was decreased from 6.8 nm for 10 % to 6.0 nm for 50 %, respectively. As seen in the SEM images, it was various tiny powders placed on the surface of the geopolymer prepared at 50 % RHA, which may act as fillers and reduce the pore size of the obtained geopolymers.

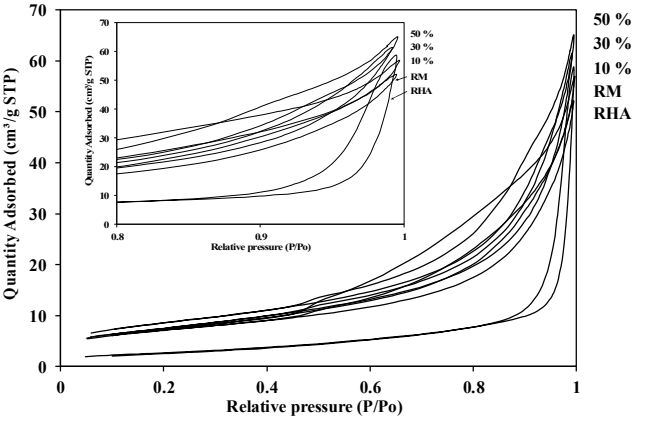

Fig. 7. The nitrogen adsorption/ desorption of initial materials and geopolymer composites

3.2.5. Zeta-potential evaluation

Fig. 8 shows the Zeta-potential as a function of pH of the different solutions of RM and RHA-based geopolymer powders. It has been known that the surface-charge of RHA was negative values in a wide range of pH from 2 to 12.[32] Therefore, the zeta potential value of RHA in this study was negative at -0.5 for pH 2 and -29.7 for pH 12. For RM and all the geopolymer composites composed of 10, 30, and 50 % RHA, it was seen that in the range of acidic pH at about 2, the surface of samples was relatively positive suggesting the potential application for the elimination of negatively charged substances such as BG ion *via* electrostatic attraction.

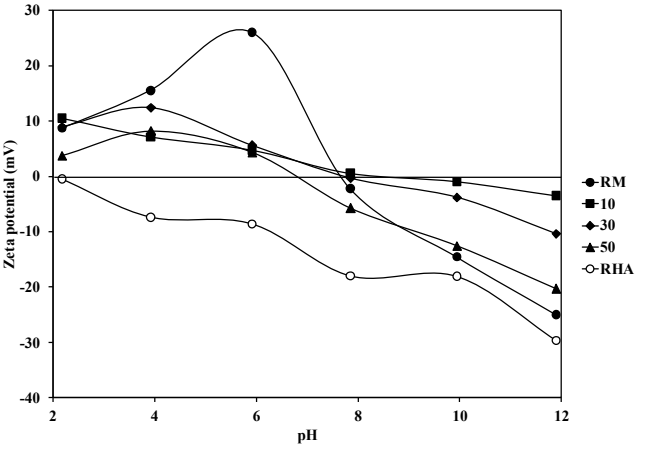

Fig. 8. Zeta-potential of the initial materials and prepared geopolymer composite

3.3. The removal experiment of bromocresol green

The value of pH was strongly considered one of the most important factors in determining the influence of the surrounding environment on the adsorption capacity of the material. At low pH and high concentration of H^+ ions, the surface of the adsorbent was positively charged. Therefore, the interaction that took place was an electrostatic attraction enhancing the adsorption capacity of BG on the surface of the material. It has been reported that the percentage of BG adsorption decreased while pH changed from 1 to 2. This result also occurred in the range of pH from 2 to 6. At pH 1, due to the excess of protons, the charge of anionic BG dye was positive, and the electrostatic attraction in comparison to pH 2 was not dominant. However, when pH was varied to 2, the positive charge of BG would be decreased, and BG interaction with the adsorbent surface increased. When the solution pH was more than 2, BG had a negative charge, and the electrostatic repulsion decreases attraction.[24] Hence, in this study, pH 2 was selected to optimize the anionic dye removal. In addition, the zeta potential results indicated that the surface charge of the prepared geopolymers at different amounts of RHA might be positive at pH 2, which was strongly considered to perform the non-protonated BG ion as well.

Herein, the effect of initial concentration on the percentage removal of BG by the mixed geopolymer powders was studied. As seen from Fig. 9a, the removal efficiency was higher than 75 % of all samples when the initial concentration of BG was 10 mg/L. Apparently, when the initial concentrations of BG were changed from 20 to 100 mg/L, the removal capacities were gradually decreased. It was because the number of adsorption sites in the geopolymer composites was able to be restricted by the increase of the BG concentration. So, at lower initial concentrations of the BG solutions, sufficient adsorption sites remained for the sorption of BG ions at pH 2, while the increasing concentration caused the reduction in uptake percentage. At higher loading of the RHA in the geopolymer composite from 10 to 50 %, the removal capacities were gradually enhanced. This might be due to increasing the sorption sites of RHA in the composite as seen in the results of surface area and pore size values. In the case of 10 % and 50 % RHA in the geopolymer composition, the value of the removal percentage increased from 67 % to 80.3 % at 40 mg/L of BG solution, respectively. However, the removal efficiency was reduced to 64.7 % and 24.7 % for the geopolymer having 50 and 10 % RHA when the excess concentration of BG was up to 100 mg/L. As seen in Fig. 9b, the initial concentration of GB had a strong effect on the binding amount of BG ion on the prepared geopolymers at different mixing ratios of RHA. A similar tendency was recorded as the concentration was changed from 10 to 100 mg/L, and the adsorption capacity gradually increased in all samples. This phenomenon indicates that higher concentrations of BG in the initial solutions may be accepted by the adsorption sites in geopolymers structures at higher RHA content. The percentage removal of GB and uptake amount are represented in Table 4.

To illustrate the relationship between the residual concentration of dye in solution and the adsorption capacity of geopolymers at a constant temperature, the Langmuir and Freundlich models were used.

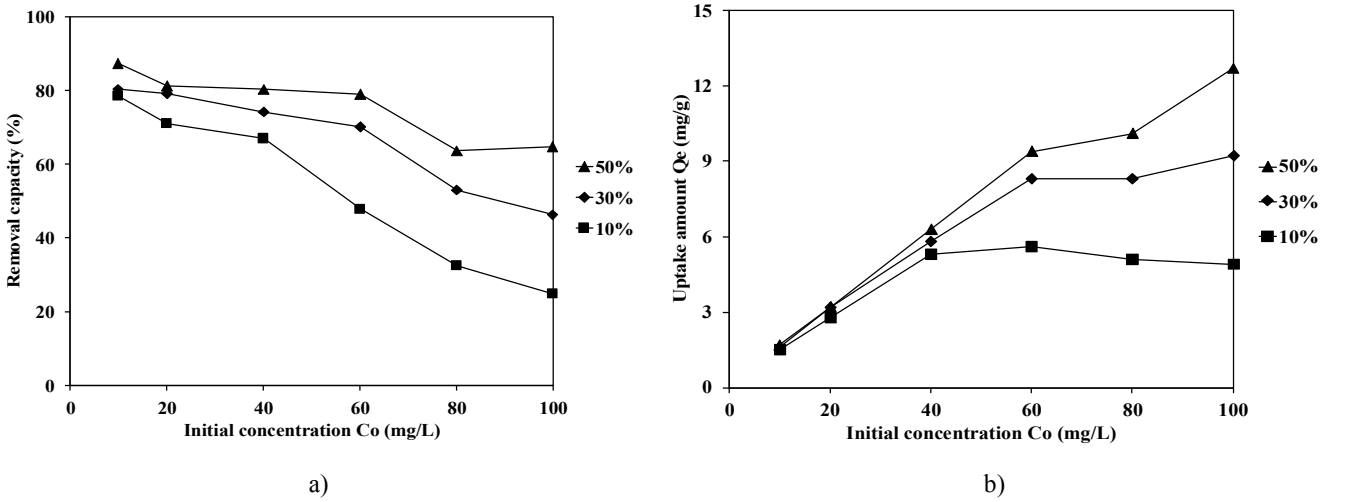

a) b)

Fig. 9. The removal capacity (%) a) and uptake amount (mg/g) b) of the geopolymer composite at different BG solutions

Table 4. The removal capacity (%) and uptake amount (mg/g) of the geopolymer composite prepared with different BG solution at pH 2

Sample	Initial concentration Co (mg/L)	Removal capacity (%)	Uptake amount Qe (mg/g)
50 %	10	87.2	1.7
	20	81.1	3.2
	40	80.3	6.3
	60	78.8	9.4
	80	63.5	10.1
	100	64.7	12.7
30 %	10	80.2	1.6
	20	79.2	3.2
	40	74.2	5.8
	60	70.1	8.3
	80	53	8.3
	100	46.1	9.2
10 %	10	78.5	1.5
	20	71	2.8
	40	67	5.3
	60	47.8	5.6
	80	32.4	5.1
	100	24.7	4.9

The linear equation of the Langmuir isotherm model was placed in the equation below:

$$\frac{C_e}{q_e} = \frac{1}{K_L q_m} + \frac{C_e}{q_m} \quad (3)$$

where, q_m (mg/g) is the maximum adsorption capacity, and K_L (L/mg) is the Langmuir constant.

In the case of Freundlich isotherm model, the linear equation was presented as follows:

$$\ln q_e = \ln K_F + \frac{1}{n} \ln C_e \quad (4)$$

where K_F (L/g) was the Freundlich isotherm constants related to the adsorption capacity and n was the adsorption strength.

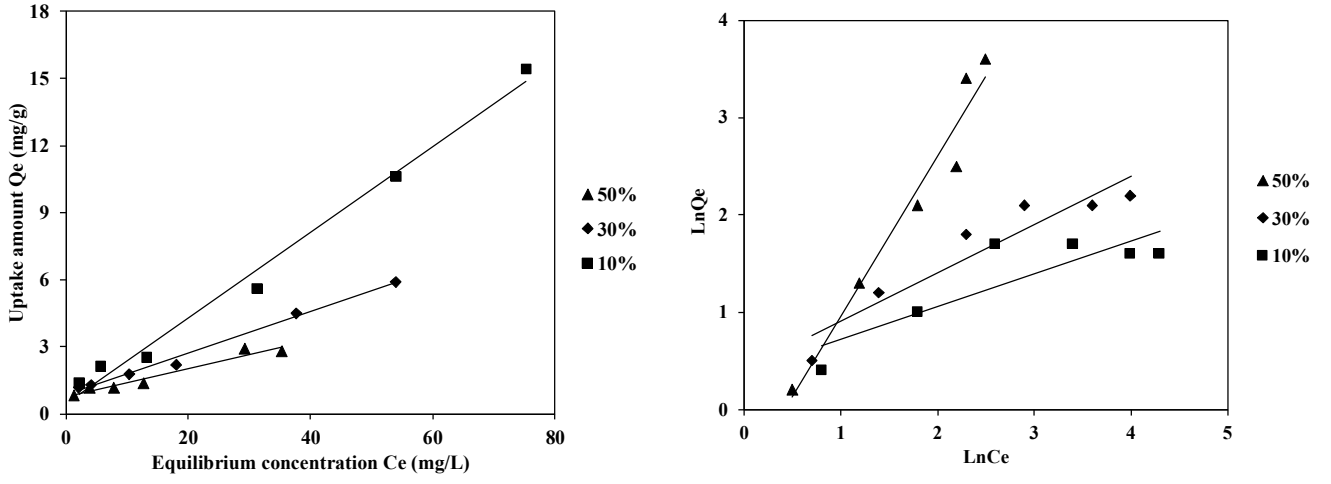

a) b)

Fig. 10. The linear Langmuir isotherm adsorption a) and Freundlich model isotherm adsorption b) of the geopolymer composite at different BG solutions

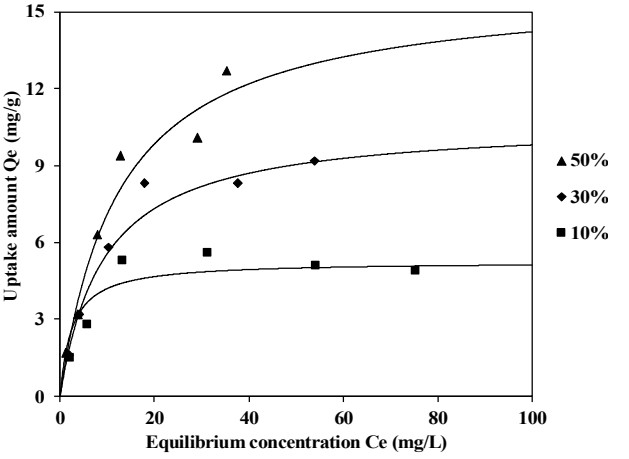

Fig. 11. The Langmuir isotherm adsorption of the geopolymer composite different BG solutions

The influence of the initial concentrations was carried out by the Langmuir and Freundlich isotherm. Based on the linear coefficients of these equations it is possible to determine how the adsorption of the RM-RHA geopolymer composites occurred. From the results of the BG adsorption amount of RM-RHA geopolymers on the effect of the initial concentrations, the adsorption isotherm was carried out to determine the parameters of the two models. As seen from the linearity of the plots in Fig. 10a, the correlation coefficient (R^2) was about 0.99 for all samples, meaning that the adsorption isotherms of BG obeyed the Langmuir model. By contrast, the lower value of R^2 calculated from the Freundlich model was 0.96 for the geopolymer prepared with 50 % RHA and 0.74 for 10 %, respectively (Fig. 10b). Therefore, the experimental results better fitted the Langmuir isotherm model than the Freundlich model, confirming that the BG adsorption onto the RM-RHA geopolymer composites was monolayer adsorption. The result suggested that the adsorption occurred on specific homogeneous sites, and all the adsorption sites were energetically identical. The result was in line with this report.[8] It was seen that the binding amount of BG ion on the samples having 50 % RHA content was higher than those of others in the adsorption test. Fig. 11 shows the adsorption isotherm of BG by the prepared geopolymer at various adding amounts of RHA at 10, 30, and 50 %. For example, when the RHA contents were increased from 10 to 50 %, the maximum binding amount of BG significantly increased to 5.24 mg/g and 16 mg/g, respectively. This result suggested that RHA was able to be a potential additive to enhance the adsorption capacity of RM-based geopolymers. The parameter values of the adsorption isotherm were placed in Table 5.

Table 5. Isotherm parameters of the BG adsorption by the RM-RHA geopolymer composite at pH 2

Sample	Parameters					
	Langmuir			Freundlich		
	q_m (mg/g)	K_L (L/mg)	R^2	1/n	K_F (L/g)	R^2
50 %	16.0	0.08	0.99	1.65	0.50	0.96
30 %	10.7	0.11	0.99	0.50	2.44	0.89
10 %	5.24	0.40	0.99	0.34	41.45	0.74

4. Conclusions

The red mud-based geopolymers were successfully prepared in the presence of different loading amounts of rice husk ash from 10 to 50 %. During the geopolymerization activated by the highly concentrated sodium hydroxide and silicate binder solution, the geopolymer linkage occurred with the addition of RHA fillers, which was confirmed by FT-IR spectra. When the content of RHA was increased from 10 % to 50 %, the surface area values of the resultant mixed geopolymers were gradually enhanced from 26.5 to 31.1 m^2/g, while the reduction in BJH pore size was recorded as 6.8 and 6.0 nm, respectively. The addition of RHA also improved the BG-uptake performance of the RM-based geopolymer. In the BG adsorption at pH 2, the results showed that the increment amount of RHA from 10 to 50 % in the geopolymer composition enhanced the adsorption capacities to 5.24 mg/g and 16 mg/g after 180 minutes, respectively. Also, the adsorption behavior of the mixed geopolymer to BG well fitted the Langmuir model, suggesting that the adsorption occurred on the homogeneous monolayer surface. This study suggests that RHA could be a useful filler to improve the uptake performance of RM-based adsorbent used in wastewater treatment.

References

[1] Gadhi, T.A.; Ali, I.; Mahar, R.B.; Maitlo, H.A.; Channa, N. Waste Heat and Wastewater Recovery in Textile Processing Industry: A Case Study of Adopted Practices. *Mehran Univ. res. j. eng. technol.* **2021**, *40*, 606–616. https://doi.org/10.22581/muet1982.2103.14

[2] Al-Tohamy, R.; Ali, S.S.; Li, F.; Okasha, K.M.; Mahmoud, Y.A.G.; Elsamahy, T.; Jiao, H.; Fu, Y.; Sun, J. A Critical Review on the Treatment of Dye-Containing Wastewater: Ecotoxicological and Health Concerns of Textile Dyes and Possible Remediation Approaches for Environmental Safety. *Ecotoxicol. Environ. Saf*. **2022**, *231*, 113160. https://doi.org/10.1016/j.ecoenv.2021.113160
[3] Nguyen Thi Phuong, L. The Status and Environmental Problems of Textile Industry. In *Environmental Governance in Asia: New State-Society Relations, NREF-AGITS Conference*; Kunphoommarl, M.; Oosterveer, P.; Sonnenfeld D.A., Eds.; Chiang Mai, 2003; pp. 245–258.
[4] Ellen MacArthur Foundation. *A new Textiles Economy: Redesigning Fashion's Future*; 2017. https://library.unccd.int/Details/fullCatalogue/1356
[5] Ito, T.; Adachi, Y.; Yamanashi, Y.; Shimada, Y. Long–Term Natural Remediation Process in Textile Dye–Polluted River Sediment Driven by Bacterial Community Changes. *Water Res*. **2016**, *100*, 458–465. https://doi.org/10.1016/j.watres.2016.05.050
[6] Berradi, M.; Hsissou, R.; Khudhair, M.; Assouag, M.; Cherkaoui, O.; El Bachiri, A.; El Harfi, A. Textile Finishing Dyes and their Impact on Aquatic Environs. *Heliyon* **2019**, *5*, e02711. https://doi.org/10.1016/j.heliyon.2019.e02711
[7] Katheresan, V.; Kansedo, J.; Lau, S.Y. Efficiency of Various Recent Wastewater Dye Removal Methods: A Review. *J. Environ. Chem. Eng*. **2018**, *6*, 4676–4697. https://doi.org/10.1016/j.jece.2018.06.060
[8] Yagub, M.T.; Sen, T.K.; Afroze, S.; Ang, H.M. Dye and its Removal from Aqueous Solution by Adsorption: A Review. *Adv. Colloid Interface Sci*. **2014**, *209*, 172–184. https://doi.org/10.1016/j.cis.2014.04.002
[9] Maleki, A.; Mohammad, M.; Emdadi, Z.; Asim, N.; Azizi, M.; Safaei, J. Adsorbent Materials Based on a Geopolymer Paste for Dye Removal from Aqueous Solutions. *Arab. J. Chem*. **2020**, *13*, 3017–3025. https://doi.org/10.1016/j.arabjc.2018.08.011
[10] Onutai, S.; Jiemsirilers, S.; Thavorniti, P.; Kobayashi, T. Aluminium Hydroxide Waste Based Geopolymer Composed of Fly Ash for Sustainable Cement Materials. *Constr. Build*. **2015**, *101*, 298–308. https://doi.org/10.1016/j.conbuildmat.2015.10.097
[11] Nguyen, K.; My, Q.N.V.; Kim, A.P.T.; Tran, P.T.; Huynh, D.; Le, O. Coal Fly Ash-Slag and Slag-Based Geopolymer as an Absorbent for the Removal of Methylene Blue in Wastewater. *Science & Technology Development Journal* **2022**, *25*, 2215–2223. https://doi.org/10.32508/stdj.v25i1.3421
[12] Matsimbe, J.; Dinka, M.; Olukanni, D.; Musonda, I. Geopolymer: A Systematic Review of Methodologies. *Materials* **2022**, *15*, 6852. https://doi.org/10.3390/ma15196852.
[13] Onutai, S.; Jiemsirilers, S.; Wada, S.; Thavorniti, P. Effect of Sodium Hydroxide Solution on the Properties of Geopolymer Based on Fly Ash and Aluminium Waste Blend. *Warasan Technol Suranaree* **2014**, *21*, 9–14.
[14] Tuyan, M.; Andiç-Çakir, Ö.; Ramyar, K. Effect of Alkali Activator Concentration and Curing Condition on Strength and Microstructure of Waste Clay Brick Powder-Based Geopolymer. *Compos. B. Eng*. **2018**, *135*, 242–252. https://doi.org/10.1016/j.compositesb.2017.10.013
[15] Pimraksa, K.; Chindaprasirt, P.; Rungchet, A.; Sagoe-Crentsil, K.; Sato, T. Lightweight Geopolymer Made of Highly Porous Siliceous Materials with Various Na_2O/Al_2O_3 and SiO_2/Al_2O_3 Ratios. *Mater. Sci. Eng. A* **2011**, *528*, 6616–6623. https://doi.org/10.1016/j.msea.2011.04.044
[16] Görhan, G.; Kürklü, G. The Influence of the NaOH Solution on the Properties of the Fly Ash-Based Geopolymer Mortar Cured at Different Temperatures. *Compos. B. Eng*. **2014**, *58*, 371–377. https://doi.org/10.1016/j.compositesb.2013.10.082
[17] Yao, X.; Zhang, Z.; Zhu, H.; Chen, Y. Geopolymerization Process of Alkali–Metakaolinite Characterized by Isothermal Calorimetry. *Thermochim Acta* **2009**, *493*, 49–54. https://doi.org/10.1016/j.tca.2009.04.002
[18] Nazari, A.; Bagheri, A.; Riahi, S. Properties of Geopolymer with Seeded Fly Ash and Rice Husk Bark Ash. *Mater. Sci. Eng. A* **2011**, *528*, 7395–7401. https://doi.org/10.1016/j.msea.2011.06.027
[19] Onutai, S.; Jiemsirilers, S.; Thavorniti, P.; Kobayashi, T. Fast Microwave Syntheses of Fly Ash Based Porous Geopolymers in the Presence of High Alkali Concentration. *Ceram. Int*. **2016**, *42*, 9866–9874. https://doi.org/10.1016/j.ceramint.2016.03.086
[20] Yu, H.; Xu, M.X.; Chen, C.; He, Y.; Cui, X.M. A Review on the Porous Geopolymer Preparation for Structural and Functional Materials Applications. *Int. J. Appl. Ceram* **2022**, *19*, 1793–1813. https://doi.org/10.1111/ijac.14028
[21] Joseph, C.G.; Taufiq-Yap, Y.H.; Krishnan, V.; Puma, G.L. Application of Modified Red Mud in Environmentally-Benign Applications: A Review. *Environ. Eng. Res*. **2020**, *25*, 795–806. https://doi.org/10.4491/eer.2019.374
[22] Fuad, M.Y.A.; Ismail, Z.; Ishak, Z.A.M.; Omar, A.K.M. Rice Husk Ash. In *Plastics Additives: An A-Z reference*; Pritchard, G., Ed.; Springer Netherlands: Dordrecht, 1998; pp 561–566. 10.1007/978-94-011-5862-6_62
[23] Costa, J.A.S.; Paranhos, C.M. Evaluation of Rice Husk Ash in Adsorption of Remazol Red Dye from Aqueous Media. *SN Appl. Sci*. **2019**, *1*, 397. https://doi.org/10.1007/s42452-019-0436-1
[24] Shokrollahi, A.; Alizadeh, A.; Malekhosseini, Z.; Ranjbar, M. Removal of Bromocresol Green from Aqueous Solution *via* Adsorption on *Ziziphus nummularia* as a New, Natural, and Low-Cost Adsorbent: Kinetic and Thermodynamic Study of Removal Process. *J. Chem. Eng. Data* **2011**, *56*, 3738–3746. https://doi.org/10.1021/je200311y
[25] Elijah, O.; Collins, O.; Okonkwo, C.; Jessica, N.-B. Application of Modified Agricultural Waste in the Adsorption of Bromocresol Green Dye. *Asian J. Chem. Sci*. **2020**, *7*, 15–24. https://doi.org/10.9734/ajocs/2020/v7i119011
[26] Perná, I.; Hanzlíček, T.; Šupová, M. The Identification of Geopolymer Affinity in Specific Cases of Clay Materials. *Appl. Clay Sci*. **2014**, *102*, 213–219. https://doi.org/10.1016/j.clay.2014.09.042
[27] Singh, S.; Aswath, M.U.; Das Biswas, R.; Ranganath, R.V.; Choudhary, H.K.; Kumar, R.; Sahoo, B. Role of Iron in the Enhanced Reactivity of Pulverized Red Mud: Analysis by Mössbauer Spectroscopy and FTIR Spectroscopy. *Case Stud. Constr. Mater*. **2019**, *11*, e00266. https://doi.org/10.1016/j.cscm.2019.e00266
[28] Adams, F.V.; Ikotun, B.D.; Patrick, D.O.; Mulaba-Bafubiandi, A.F. Characterization of Rice Hull Ash and Its Performance in Turbidity Removal from Water. *Part. Sci. Technol*. **2014**, *32*, 329–333. https://doi.org/10.1080/02726351.2013.867001
[29] Rahman, M.M.; Muttakin, M.; Pal, A.; Shafiullah, A.Z.; Saha, B.B. A Statistical Approach to Determine Optimal Models for IUPAC-Classified Adsorption Isotherms. *Energies* **2019**, **12**, 4565. https://doi.org/10.3390/en12234565.
[30] Donohue, M.D.; Aranovich, G.L. Classification of Gibbs Adsorption Isotherms. *Adv. Colloid Interface Sci.* **1998**, *76-77*, 137–152. https://doi.org/10.1016/S0001-8686(98)00044-X
[31] Kumar, K.V.; Gadipelli, S.; Wood, B.; Ramisetty, K.A.; Stewart, A.A.; Howard, C.A.; Brett, D.J.L.; Rodriguez-Reinoso, F. Characterization of the Adsorption Site Energies and Heterogeneous Surfaces of Porous Materials. *J. Mater. Chem. A* **2019**, *7*, 10104–10137. https://doi.org/10.1039/C9TA00287A

[32] Liou, T.-H.; Liou, Y.H. Utilization of Rice Husk Ash in the Preparation of Graphene-Oxide-Based Mesoporous Nanocomposites with Excellent Adsorption Performance. *Materials* **2021**, *14*, 1214. https://doi.org/10.3390/ma14051214.

Received: May 24, 2023 / Revised: June 27, 2023 / Accepted: September 29, 2023

ОДЕРЖАННЯ ТА ХАРАКТЕРИСТИКА ГЕОПОЛІМЕРУ НА ОСНОВІ ЧЕРВОНОГО ШЛАМУ З ДОДАВАННЯМ ЗОЛИ РИСОВОГО ЛУШПИННЯ ДЛЯ АДСОРБЦІЇ БРОМКРЕЗОЛОВОГО ЗЕЛЕНОГО У ВОДНОМУ РОЗЧИНІ

Анотація. *Промислові відходи на основі геополімерів у формі червоного шламу (ЧШ) були успішно отримані в присутності різної кількості золи рисового лушпиння (ЗРЛ). Під час приготування варіювали кількість доданої в геополімерну композицію ЗРЛ від 10 до 50 % за масового співвідношення розчину в'яжучої речовини (Na_2SiO_3) і активованого розчину лужного металу (NaOH 7 М) 2,5, а умови затвердіння фіксували за 333 К протягом 24 год. Для характеристики оцінювали морфологію поверхні за допомогою сканувального електронного мікроскопа (SEM), оснащеного енергодисперсійною рентгенівською камерою, яка виявляла розподіл елементів до і після геополімеризації. Для встановлення утворення геополімеру використовували інфрачервону спектроскопію з Фур'є-перетворенням (FT-IR). Вплив кількості ЗРЛ на величину питомої площі поверхні за методом Брунауера-Еммета-Теллера (БЕТ) і розмір пор за методом Барретта-Джойнера-Галенди (ВЈН) отриманих геополімерів визначали за допомогою приладу для адсорбції газоподібного азоту. В адсорбції бромкрезолового зеленого (БЗ), яку проводили за pH 2, вищий вміст ЗРЛ у складі геополімеру збільшував адсорбційну здатність протягом 180 хвилин. Крім того, поведінка адсорбції змішаного геополімеру щодо БЗ добре узгоджується з моделлю Ленгмюра, вказуючи на те, що адсорбція відбувається на однорідній моношаровій поверхні геополімеру. З цього дослідження випливає, що ЗРЛ може бути природним потенційним наповнювачем для покращення поглинання БЗ геополімером на основі ЧШ в очищенні стічних вод.*

Ключові слова: *адсорбція барвника, геополімер, бромкрезоловий зелений, червоний шлам, зола рисового лушпиння.*